ELSEVIER

Fish & Shellfish Immunology 22 (2007) 327–339

Fish & Shellfish Immunology

www.elsevier.com/locate/fsi

Lysozyme gene expression by hemocytes of Pacific white shrimp, *Litopenaeus vannamei,* after injection with *Vibrio*

Erin J. Burge*, Daniel J. Madigan, Louis E. Burnett, Karen G. Burnett

Grice Marine Laboratory, College of Charleston and Hollings Marine Laboratory, 331 Fort Johnson Road, Charleston, SC 29412, USA

Received 25 April 2006; revised 8 June 2006; accepted 9 June 2006
Available online 15 June 2006

Abstract

The purpose of this study was to quantify the gene expression of lysozyme, an important antibacterial protein produced by shrimp hemocytes, within tissues of *Litopenaeus vannamei* Boone in response to a pathogen challenge. We quantified lysozyme transcripts with a real-time PCR method and used these data, along with total hemocyte counts, to infer patterns of hemocyte trafficking during the immune response. Transcript expression was detected by in situ hybridization of mRNA in circulating hemocytes, and within tissues with high hemocyte concentrations. Lysozyme gene expression was monitored in 5 tissues and in circulating hemocytes for 48 h following challenge with the shrimp pathogen *Vibrio campbellii* Baumann. The results suggest that lysozyme is expressed in most if not all hemocytes in circulation and in peripheral tissues. Injection with *V. campbellii* produced a significant decrease in transcriptional signal in circulating hemocytes and peripheral tissues 4 h after injection. Over the same early time period lysozyme signal increased significantly in the muscle at the site of injection and remained high for the duration of the time-course, suggesting that hemocytes are recruited to the site of injection early during the course of the immune response. After 4 h, lysozyme signal increased in circulating hemocytes and tissues, with a return to control levels noted for all tissues except the muscle at the site of injection.

Keywords: *Litopenaeus vannamei*; Shrimp; Hemocyte; *Vibrio*; Lysozyme; Gene expression; Quantitative real-time PCR; Lymphoid organ; In situ hybridization

1. Introduction

The Pacific white shrimp, *Litopenaeus vannamei* Boone, is one of the predominant shrimp species produced in aquaculture. Economic losses due to disease in shrimp aquaculture have made it necessary to increase our knowledge of the invertebrate immune system, identify the major molecular mediators of innate immunity, and unravel the mechanisms of pathogenicity. The purpose of this study was to examine the gene expression of lysozyme, an important antibacterial protein produced by shrimp hemocytes, within tissues of *L. vannamei* in response to a pathogen challenge.

Hemocytes are the primary mediators of cellular immune responses in decapod crustaceans. Functional roles of hemocytes include non-self recognition [1], phagocytosis [2], reactive oxygen intermediate production [3], wound

* Corresponding author. Tel.: +1 843 349 6491; fax: +1 843 349 2545.
E-mail address: eburge@coastal.edu (E.J. Burge).

1050-4648/$ - see front matter © 2006 Elsevier Ltd. All rights reserved.
doi:10.1016/j.fsi.2006.06.004

repair [4], and melanization with encapsulation of foreign materials [2, 5]. Crustacean hemocytes are also recognized for their important role in the removal of foreign bodies from the host [2, 6–9]. The total numbers of circulating hemocytes rapidly decline (within minutes) in response to bacterial injection [2, 9, 10], but it remains unclear whether hemocytes are lysed in vivo or migrate into certain tissue compartments where they undergo differentiation, and are no longer recognizable as freely circulating hemocytes [9, 11]. Martin et al. [2] depleted circulating hemocytes by bacterial injection and determined that a second bacterial challenge administered 24 h later was cleared at the same rate, suggesting that non-circulating or tissue-fixed hemocytes have continued bactericidal activity. Muñoz et al. [12] observed a dramatic increase from 3 to 6 h in immunoreactivity of a hemocyte-specific antimicrobial peptide (penaeidin 3a) at the intramuscular site of injection of *Vibrio penaeicida* into *L. vannamei* that they ascribed to hemocyte chemotaxis to the site of injury and infection. Additionally, they reported large decreases in both circulating and tissue-infiltrated hemocyte numbers during the same time frame. Much effort has been expended to differentiate crustacean hemocytes morphologically [11, 13], functionally [14], and antigenically [15–18], with recent activities focused on identifying hemocyte-specific genes that define specific blood cell subpopulations [19–21].

Antibacterial c-type lysozyme catalyzes cell wall hydrolysis against bacteria [22], and acts as a nonspecific immune defense in penaeid shrimp [23–25]. Penaeid shrimp lysozymes are well characterized, hemocyte-specific proteins that have been shown to possess lytic activity against a range of Gram positive and Gram negative bacterial species, including pathogenic *Vibrio* spp. [23, 25]. Lysozyme enzymatic activity was specific to hemocyte lysate, being absent in cell-free hemolymph, and was estimated to comprise approximately 4% of the total hemocyte protein pool in *L. vannamei* [24]. Lysozyme gene expression by reverse transcription polymerase chain reaction (RT-PCR) in hemocytes has been reported [24], although it was not stated whether other tissues were tested. Hikima et al. [25] reported that lysozyme from *Marsupenaeus japonicus* was strongly expressed by RT-PCR in samples from hemocytes, moderately expressed in the epidermis, and weakly expressed in the gills, midgut and muscle. Subtractive suppression hybridization with hemocyte cDNAs isolated from *L. stylirostris* surviving infection with *V. penaeicida* yielded a lysozyme EST and information about the post-infection expression profile [26]. Subsequent macroarray, Northern blot, and real-time PCR analysis revealed that hemocyte lysozyme expression during *V. penaeicida* challenge was significantly lower at 12 h post-infection and had returned to control levels within 24–96 h post-challenge in surviving shrimp. Shrimp that did not survive infection expressed very low levels of lysozyme 24 h after infection [26].

The purpose of the present study was to profile the change in the number and distribution of hemocyte lysozyme transcripts in shrimp tissues in response to injection of bacteria. Real-time PCR was used to quantify lysozyme transcripts in tissues after bacterial challenge. In situ hybridization confirmed the specificity of lysozyme expression to hemocytes, and yielded insights about tissue level localization of hemocytes during the immune response to bacteria.

2. Materials and methods

Unless otherwise noted all reagents and chemicals were purchased from Sigma–Aldrich (St. Louis, MO).

2.1. Animal collection and maintenance

Pacific white shrimp, *L. vannamei* Boone ($n = 84$, 19.6 ± 2.5 g) were obtained from the South Carolina Department of Natural Resources, Waddell Mariculture Center, Bluffton, South Carolina, and housed at the Hollings Marine Laboratory, Charleston, South Carolina. Shrimp were kept in recirculating seawater at 30 ± 2 ppt salinity, 22–25 °C and pH > 7.8. Animals were fed once daily with commercial shrimp feed (Quality Aquaculture Feed, Rangen Inc., Buhl, ID). Water quality was checked daily, and feeding was stopped 24 h before treatment. Animals were held for a minimum of 2 weeks prior to experimental use.

2.2. Vibrio growth and bacterial challenge

The 90-69B3 strain of *Vibrio campbellii* Baumann was originally isolated from diseased *L. vannamei* by D. Lightner and L. Mahone, University of Arizona, and modified by conjugation to harbor a plasmid coding for kanamycin and chloramphenicol antibiotic resistance, and to express green fluorescent protein (GFP) [6, 27]. In our laboratory, the *V. campbellii* LD_{50} for *L. vannamei* was determined to be 3.06×10^5 colony forming units (CFU)/g shrimp [28]. This *Vibrio* species is routinely isolated from both clinically healthy and diseased animals, plus their husbandry

facilities, throughout the world [29]. For each injection, *V. campbellii* from a single working stock was streaked onto Tryptic Soy Agar (TSA) plates supplemented with 2.5% NaCl and 100 μg mL^{-1} kanamycin A, and then grown overnight at 25 °C.

Bacterial injection doses were prepared as previously described in Ref. [6]. Experimental treatments for the time-course of lysozyme expression consisted of an intramuscular injection of 2×10^4 viable *V. campbellii* g^{-1} shrimp into the third abdominal segment. Injection volumes for this experiment were 0.5 μL g^{-1} shrimp of 4×10^7 CFU mL^{-1} diluted in sterile HEPES-buffered saline. This injection dose of bacteria is approximately 10% of the LD_{50} dose for *L. vannamei* [28] and was used to profile a ''successful'' immune response. Control-injected animals received an equivalent intramuscular injection of 0.5 μL g^{-1} shrimp of sterile HEPES-buffered saline.

2.3. Experimental conditions

Animals for the lysozyme expression time-course were transferred from their holding tanks into 19 L glass aquaria fitted with recirculating water pumps routed through a biologically charged trickle filter with vigorous aeration. Immediately before being placed in the treatment tanks, individual shrimp were weighed (nearest 0.1 g) and injected with sterile HEPES-buffered saline or the correct bacterial suspension volume to achieve 2×10^4 CFU g^{-1} shrimp. Two animals were housed per tank and simultaneous control (saline; $n = 37$, 4–6 animals per time-point) and *Vibrio*-injected ($n = 37$, 4–6 per time-point) animals were held in separate tanks. At predetermined times after injection (either 0.25, 1, 4, 12, 24 or 48 h) shrimp were removed from the challenge tanks and dissected. No mortalities were recorded for either injection group in these experiments. Each tank was cleaned, bleached and rinsed between each pair of shrimp.

2.4. Hemolymph and tissue sampling

At the appropriate time-points, shrimp were removed from tanks and hemolymph was extracted into 3 volumes of ice-cold shrimp anticoagulant solution (SACS) [30] by bleeding into a preweighed (nearest 0.001 g) 1 mL syringe tipped with a 26 gauge needle. Shrimp were bled from the hemolymph sinus at the base of each walking leg. A small (50 μL) subsample was immediately mixed with an equal volume of 10% neutral-buffered formalin (10% NBF) for determination of total circulating hemocyte count mL^{-1} (THC). The remainder of the hemolymph SACS was briefly centrifuged, the hemolymph supernatant removed, and the hemocyte pellet resuspended in 500 μL RNAlater™ solution (Ambion Inc., Austin, TX). Gill tissue (one side only), heart, hepatopancreas, lymphoid organ, and muscle at the injection site were dissected and placed in 1 mL RNAlater™. Tissues and hemocytes were held overnight at 4 °C and stored at −20 °C prior to RNA extraction, as per the manufacturer's instructions.

2.5. RNA preparation

Tissue and hemocyte samples were extracted for total RNA using the RNeasy® Mini Kit (Qiagen Inc., Valencia, CA). Gill, hepatopancreas, and muscle were subsampled to 20–30 mg tissue prior to extraction. Tissue samples were homogenized in 600 μL of the supplied lysis buffer using a Tissue-Tearor™ power homogenizer (Biospec Products, Inc., Bartlesville, OK), treated with RNase-free DNase on a silica-gel column, and eluted in 25–30 μL RNase-free water. Isolated total RNA was stored at −80 °C until reverse transcription and real-time PCR analysis. RNA sample concentrations and purity were measured spectrophotometrically at 260 nm and corrected for protein contamination at 280 nm.

2.6. Reverse transcription

Due to the need to maintain archival cDNA samples for later analysis and the low amount of recovered RNA from tissues, total RNA from this experiment was reverse transcribed separately, prior to real-time PCR determination. Briefly, 100–2000 ng of total RNA was reverse transcribed using the Omniscript® Reverse Transcription Kit (Qiagen Inc., Valencia, CA) following the manufacturer's protocol for first-strand cDNA synthesis from animal cells for 2-tube real-time RT-PCR. First-strand synthesis was accomplished using final concentrations of 1× RT buffer, 2 U μL^{-1} RNase inhibitor, 0.5 mM of each dNTP, 0.2 U μL^{-1} Omniscript® reverse transcriptase, primed with 1 μM oligo

dT_{16}, and 10 μM random nonamers in a final reaction volume of 20 μL. Archival cDNA samples were prepared in 96-well PCR reaction plates (1 per tissue) and stored at −20 °C until quantified by real-time PCR.

2.7. Real-time PCR

Real-time PCR was performed by an Applied Biosystems (Foster City, CA) 7500 Sequence Detection System (software version 1.2.3) using QuantiTect™ Probe PCR kits (Qiagen Inc., Valencia, CA). Forward primer Lv lys 254F (5′-GCA AGA ACG TCT GCA AAA TCC-3′), reverse primer Lv lys 444R (5′-CCA GCA CTC TGC CAT GTA CTG-3′), and dual-labeled hybridization probe Lv lys 280P (5′-TCC GAT CTG ATG TCC GAT GAT ATC ACG-3′), 5′ fluorophore-labeled with 6-carboxyfluorescein and 3′ quencher-labeled with Black Hole Quencher-1™, were used for all amplifications (Integrated DNA Technologies, Coralville, IA). These oligonucleotides were developed using Applied Biosystems Primer Express v. 2.0.0 software on the sequence for *L. vannamei* lysozyme (accession number AF425673) available on GenBank [24], and produced a 190 bp amplicon. Reactions consisted of final concentrations of 1/20 volume (1 μL) of cDNA, 0.2 μM per primer, 0.4 μM dual-labeled hybridization probe, and QuantiTect™ Probe PCR kit HotStarTaq DNA polymerase with dNTPs in an appropriate buffer system in a final volume of 25 μL. Duplicate reactions were examined for each sample and standard. Positive control reactions consisted of a standard curve of known concentrations (10^8–10^2 molecules μL^{-1}) of a 460 bp in vitro transcribed *L. vannamei* lysozyme RNA supplemented with 20 ng μL^{-1} *Fundulus heteroclitus* liver total RNA [31]. Standard curves were generated for each set of real-time PCR reactions. Negative control reactions were run in parallel, omitting template cDNA. Thermocycling parameters consisted of 15 min denaturation and HotStarTaq activation at 95 °C, followed by 40 cycles of 94 °C for 15 s and 60 °C for 1 min. Fluorescence emission was monitored during the 60 °C annealing/extension step by the real-time PCR instrument. Sample absolute lysozyme concentrations were determined by interpolation using the linear regression equation derived from the known standards for each reaction and normalized to lysozyme transcripts ng^{-1} total RNA using the predetermined total RNA concentrations for each sample.

2.8. In situ hybridization

Tissue- and cell-level expression of lysozyme transcripts in *L. vannamei* was evaluated using in situ hybridization on paraffin-embedded tissue sections hybridized with digoxin-labeled antisense oligonucleotide probes. This in situ hybridization procedure was based on protocols developed for *Cancer magister* by Terwilliger et al. [32]. Tissues (gill, heart, hepatopancreas, lymphoid organ, and muscle) were aseptically dissected from healthy control animals from the same stocks from which experimental animals were selected. Dissected tissues were immediately fixed in 10 volumes of RF fixative [33] overnight at room temperature. Hemolymph was bled into 5 volumes of 10% NBF, centrifuged immediately, and the resulting hemocyte pellet was resuspended in 15 mL of 10% NBF for overnight fixation at 4 °C. Tissues were transferred to 70% ethanol and then serially dehydrated by 30 min incubations of 10 volumes of 85%, 95%, 100%, and 100% ethanol followed by 2 xylene washes. Dehydrated tissues were incubated for 30 min in 60 °C xylene:paraffin, vacuum-infiltrated 45 min and embedded in cassettes. Tissues were sectioned (5–7 μm) on a rotary microtome (American Optical Model 820), mounted on Fisher Superfrost Plus slides (Fisher Scientific, Pittsburgh, Pennsylvania), air-dried 1 h, and baked at 40 °C overnight. Formalin-fixed hemocytes were centrifuged for 10 min at 800 *g*, washed once in 70% ethanol and resuspended in 70% ethanol to 1×10^7 hemocytes mL^{-1}. Five microliter drops of the hemocyte suspension was applied to Fisher Superfrost Plus slides and allowed to air-dry for 1 h. Long-term storage of slides was at 4 °C.

Tissue sections were dewaxed in 2 xylene washes and rehydrated through a graded series of ethanol washes, DEPC-treated water and DEPC–PBS. Sections were post-fixed in 4% paraformaldehyde and acetylated with 2 washes of 0.1 M triethanolamine buffer containing 0.25% acetic anhydride. Tissue sections were permeabilized at 37 °C for 10–30 min with 5–20 μg mL^{-1} PCR-grade recombinant proteinase K (Roche Applied Science, Penzburg, Germany). Hemocyte smears and tissue sections were washed twice in 2× SSC prior to prehybridization. Prehybridization was 2 h at 37 °C in hybridization buffer containing 50% deionized formamide, 2× SSC, 1× Denhardt's solution, 10% dextran sulfate, 50 mM phosphate buffer (pH 7.0), 100 mM DTT, 250 μg mL^{-1} yeast tRNA, 250 μg mL^{-1} polyadenylate nucleotides, and 500 μg mL^{-1} denatured, sheared salmon sperm DNA. Positive control (50 ng mL^{-1} GreenStar*™ digoxin-labeled poly dT_{48} hybridized; GeneDetect.com Ltd., Auckland, New Zealand) sections and

hemocyte smears were prehybridized at room temperature in hybridization buffer without the polyadenylate reagent. Hybridization occurred at 37 °C (room temperature for poly dT_{48} probe) for 18 h in a humid chamber with 200 ng mL^{-1} GreenStar*™ digoxin-labeled 48 mer antisense oligonucleotide probe 5′-(CGG CCG TGT TGA AGG ACG ACT CGA ACT CCG CGA TGC ACA CCC AGT TCT). A GreenStar*™ digoxin-labeled sense probe (200 ng mL^{-1}) was used as a negative control to ensure specific target binding of the antisense probe.

After hybridization, repeated stringency washes in 1× and 0.5× SSC were conducted at 55 °C (poly dT_{48} probe washes were at room temperature). Hybridized sections and hemocyte smears were blocked for 30 min with 1× blocking reagent (Roche Applied Science, Penzburg, Germany) in TBS. Hybridized sections and hemocyte smears were detected with alkaline phosphatase-conjugated anti-digoxigenin Fab fragments (Roche Applied Science, Penzburg, Germany) at 100 ng mL^{-1} in 1× blocking reagent. Purple-blue NBT/BCIP staining (BM Purple AP substrate, precipitating; Roche Diagnostics, Indianapolis, IN) was used to visualize the probe:antibody complexes. Sections and hemocyte smears were mounted with Crystal/Mount aqueous mounting medium (Biømeda Corp., Foster City, CA) prior to examination by light microscopy.

2.9. Data analysis

To determine the contribution of each variable (THC, tissue type, treatment, time) to the observed variation between and within animals, the lysozyme time-course data were analyzed initially by developing a set of artificial neural networks (ANN) ($n = 10$) using WebNeuralNet 1.0 [34]. Each of the ANNs consisted of 9 input variables and 1 output variable ($\log_{10}$ real-time PCR lysozyme data). Data and input variables were coded prior to analysis, with tissue type (gill, heart, hemocytes, hepatopancreas, lymphoid organ or muscle) and treatment (saline or *Vibrio* injected) expressed on a binary scale, time (h) as a $\log_2$ value, and $\log_{10}$-transformed THC and real-time PCR values. Each ANN was developed using a random sample of 378 of 423 real-time PCR and THC data points. After each ANN was trained, the 45 withheld data points were analyzed to evaluate the predictive capabilities of the ANN. Outputs from each ANN consisted of a correlation coefficient and distribution of sensitivity values for each input variable.

Subsequently, the $\log_{10}$ lysozyme data for each tissue within an individual were normalized to the individual's average $\log_{10}$ lysozyme concentration over all tissues, and a 3-way mixed model analysis of variance (ANOVA, $\alpha = 0.05$) was applied to the data in the R 1.9.1 statistical package [35]. Individual tissue, treatment and time-point effects were analyzed by 2-factor ANOVA ($\alpha = 0.05$) and multiple comparisons performed using the post hoc Holm–Sidak test in Sigma Stat 3.1 (SPSS, Chicago, IL).

3. Results

3.1. Specificity of lysozyme transcription by in situ hybridization

Cellular lysozyme expression in circulating hemocytes and isolated tissues was examined by in situ hybridization of uninjected shrimp (Fig. 1). Hyaline, semigranular, and granular hemocytes were hybridized with the lysozyme antisense hybridization probe, with granular cells displaying the most intense staining (Fig. 1A and B). Hyaline-like cells exhibited the least staining but were readily distinguished from non-stained cells in negative control (lysozyme sense hybridization probe) preparations. In circulating hemocytes, the lysozyme antisense hybridization probe was bound to subcellular granules or other intracellular particles (Fig. 1B).

Among the tissues examined, lysozyme transcripts were located exclusively in cells that morphologically resembled hemocytes. The antisense probe detected foci of lysozyme expression within certain tissues, especially the heart (Fig. 1C and D) and lymphoid organ (Fig. 1E and F). The periphery of the lymphoid organ tubules stained intensely, most often in regions that had many interstitial sinuses. Hemocytes within the tubule lumen itself exhibited variable staining intensity, but were usually readily distinguishable from the background. Within the heart, positively staining hemocytes were most often associated with the hemolymph spaces of the lumen and within channels between the muscle bands. Large numbers of hemocytes were expected to be present in the gills (Fig. 1G), but few cells were observed. When detected within the gill lamellae, hemocytes were morphologically similar to circulating hemocytes. These cells stained positive for lysozyme transcripts and were most often detected at the distal tips of individual gill filaments. Positively staining cells were rarely observed within muscle tissue of uninjected shrimp (Fig. 1H), although when

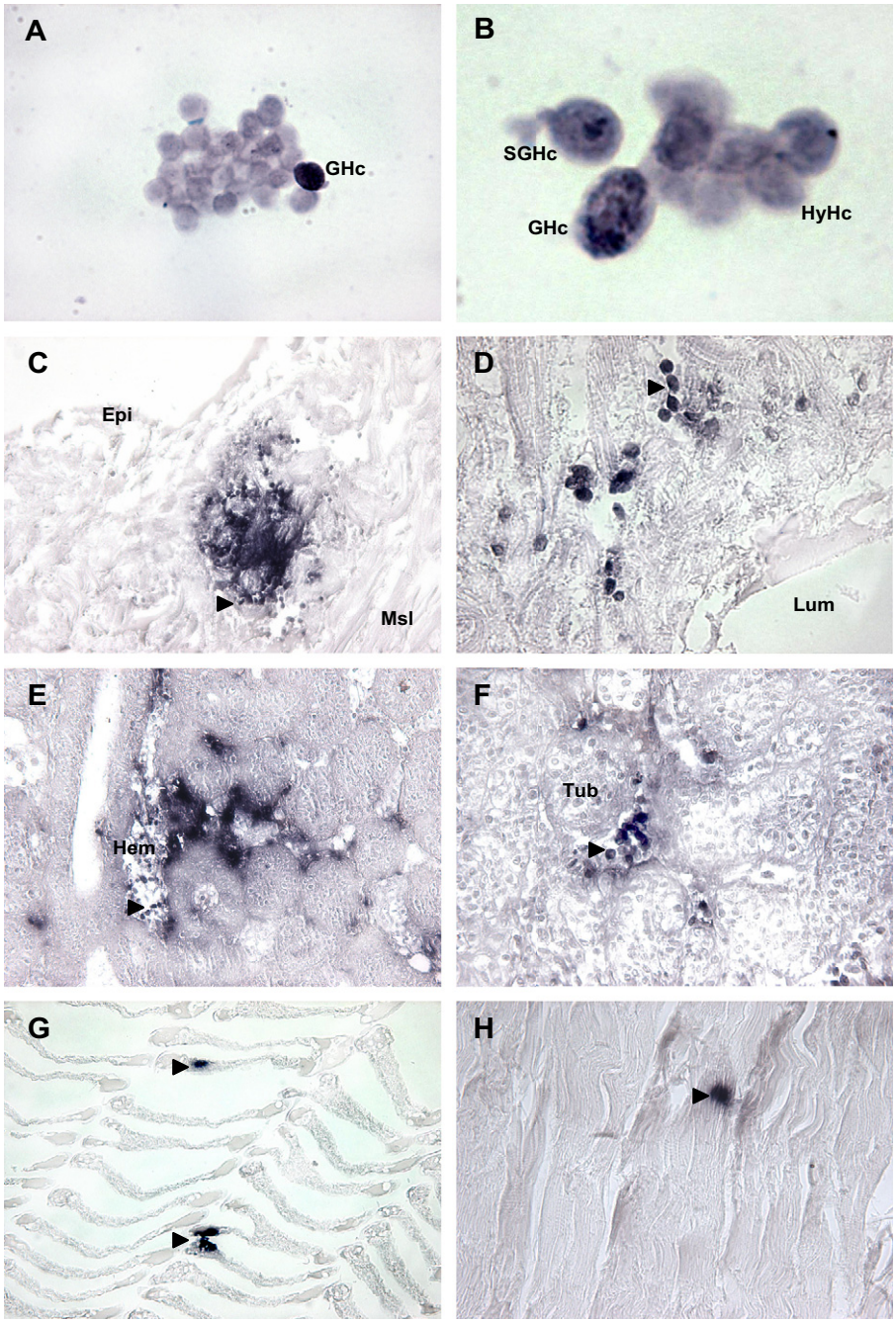

Fig. 1. In situ hybridization. In situ hybridization was used to assess the tissue and cellular expression of lysozyme mRNA transcripts using a digoxin-labeled *L. vannamei* lysozyme-specific antisense oligonucleotide probe. Tissues and circulating hemocytes are from uninjected control animals. Positive hybridization was observed especially for granular hemocytes in circulation, with other morphological subtypes displaying reduced signal intensity. Arrowheads indicate hemocytes within tissues. (A) Aggregation of circulating hemocytes (600×), GHc granular hemocyte; (B) hemocyte subtypes (1000×), SGHc semi-granular hemocyte, HyHc hyaline or agranular hemocyte; (C) heart section (200×) showing intense staining within a hemolymph sinus, Hem, Epi epicardium, Msl cardiac muscle; (D) higher magnification (400×) micrograph of heart indicating the lumen (Lum), and hemocytes within a vascular channel; (E) section showing lymphoid organ (200×) tissue structure and cross sections of tubules with positive staining of hemocytes along the periphery, a hemolymph sinus is indicated (Hem); (F) higher magnification of lymphoid organ (400×) with a tubule (Tub) indicated; (G) longitudinal section of gill filaments (400×) showing positive hemocyte hybridization; (H) muscle tissue (600×) with an infiltrating hemocyte noted. Positive and negative control sections (data not shown) confirmed the specificity of in situ hybridization signals.

observed, they were often intensely stained and appeared to be circulating hemocytes that had infiltrated between the muscle fibers.

Hybridization with a digoxin-labeled poly dT_{48} probe as a positive control demonstrated that intact mRNA was present in tissue sections and isolated hemocytes (data not shown). Negative control sections and circulating hemocytes hybridized with a lysozyme sense probe did not exhibit any staining when processed simultaneously with positive control and experimental samples, demonstrating the specificity of the antisense lysozyme probe for in situ hybridization (data not shown).

3.2. Response of circulating hemocytes to challenge with V. campbellii

In *Vibrio*-injected animals ($n = 37$, 19.36 ± 2.61 g) total hemocyte counts (THC) declined to approximately 45% of pre-injection values ($1.82 \times 10^7 \pm 2.99 \times 10^7$ hemocytes mL^{-1} hemolymph) within 4 h and continued to decline to 23% of pre-injection levels by 48 h after treatment (Fig. 2). THC in saline-injected animals ($n = 37$, 19.91 ± 2.44 g) also declined to approximately 63% of pre-injected values by 4 h, but remained at that level for the duration of the 48 h experiment (Fig. 2). Treatment and time-point after injection significantly affected THC ($p < 0.001$; 2-way ANOVA), but a significant difference ($p = 0.01$) was noted only at 48 h post-challenge in post hoc pairwise comparison between *Vibrio*- and saline-injected animals (Holm–Sidak multiple comparison).

The abundance of lysozyme transcripts (transcript number ng^{-1} total RNA) in circulating hemocytes of *Vibrio*-injected animals decreased over the first 4 h of the experiment ($p \leq 0.01$; 2-way ANOVA) along with the decline in THC (Fig. 3; Hemolymph), then rebounded to preinjection values by 48 h after injection, even though THC continued to decline. The abundance of lysozyme transcripts in circulating hemocytes of saline-injected shrimp did not change significantly over the entire experiment.

3.3. Lysozyme expression in tissues after V. campbellii injection

In all tested tissues except hepatopancreas, patterns of lysozyme expression through time differed strikingly between *Vibrio*- and saline-injected animals (Fig. 3). For saline-injected animals the number of lysozyme transcripts ng^{-1} RNA in the gills, heart, lymphoid organ and muscle remained the same or increased slightly between 0.25 and

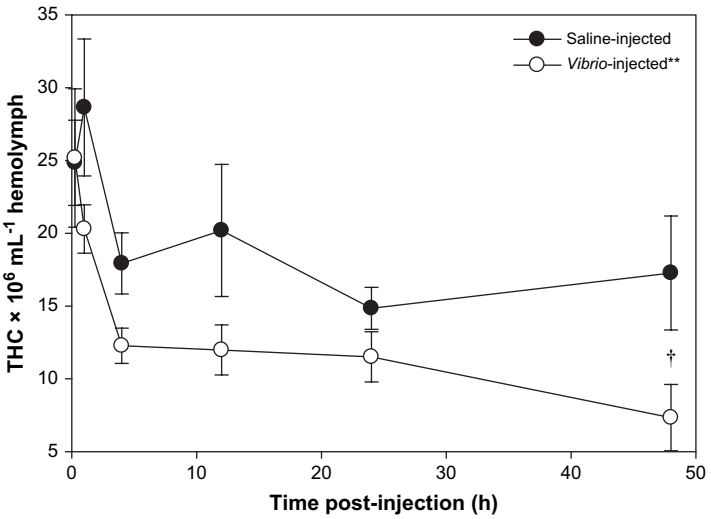

Fig. 2. Total hemocyte counts. Mean total circulating hemocyte count mL^{-1} hemolymph (THC) ± SE from control saline- ($n = 37$) and *Vibrio*-injected ($n = 36$) shrimp. *Vibrio*-injected shrimp had significantly lower (2-way ANOVA, $^{**}p \leq 0.01$) THC. Pre-injected shrimp THC (data not shown; $n = 10$) was $1.82 \times 10^7 \pm 2.99 \times 10^7$ hemocytes mL^{-1} hemolymph. A significant time-point effect in aggregate was detected in the analysis ($p < 0.01$), but significant differences were not detected in pairwise comparisons (Holm–Sidak) at each time-point except at 48 h post-challenge ($^{\dagger}p = 0.01$) between saline- and *Vibrio*-injected animals.

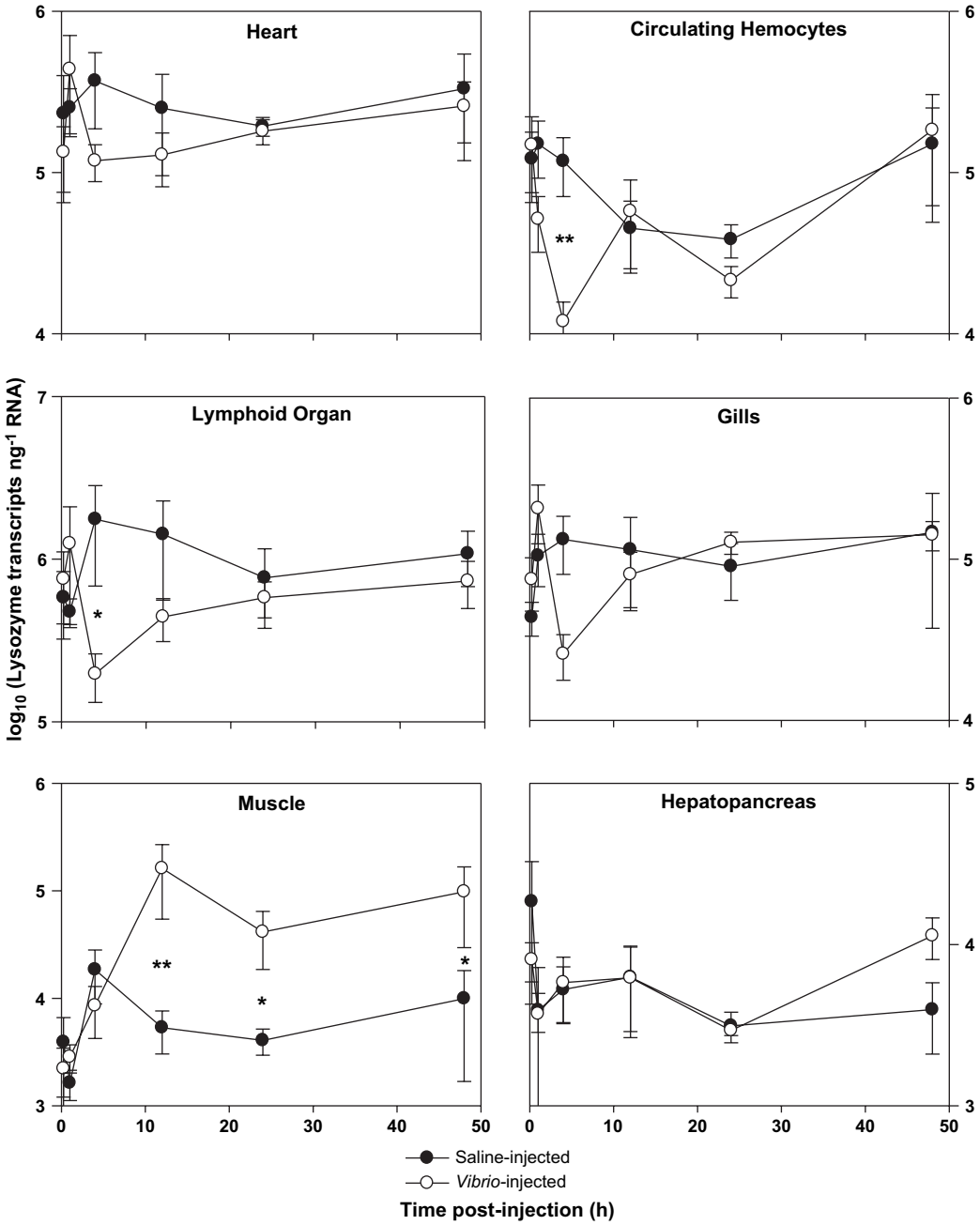

Fig. 3. Time-course of lysozyme expression by hemocyte-infiltrated tissue. Real-time PCR calculated $\log_{10}$ (lysozyme transcripts ng^{-1} RNA $\pm$ SE) are shown from 0.25 to 48 h after control (saline) or *Vibrio* injection. To conduct the full data set analysis using a 3-way mixed model ANOVA, a mean $\log_{10}$ lysozyme value for each individual was calculated and tissue levels were adjusted by subtracting the mean $\log_{10}$ value from each of the measured tissue values. This normalization served to baseline each animal and enable inter-animal comparisons. The 3-way ANOVA indicated that there was a significant difference due to tissue type ($p < 0.001$) and a significant effect due to *Vibrio* injection ($p = 0.0341$). This analysis was unable to detect time-point-specific differences because of the nonlinear nature of the lysozyme expression response. Significant differences between time-points for control and *Vibrio*-injected animals were assessed by analyzing each tissue separately using 2-way ANOVA. Significant differences in treatments were detected for 4 h post-injection in the circulating hemocytes and lymphoid organ and from 12 to 48 h for the muscle (*$p \leq 0.05$, **$p \leq 0.01$).

4 h and remained at these initial levels without significant change through the duration of the experiment, as was noted above for the circulating hemocytes of the hemolymph. In contrast, lymphoid organs from *Vibrio*-injected animals contained significantly fewer lysozyme transcripts by 4 h post-injection ($p \leq 0.05$; 2-way ANOVA), mirroring the changes seen in circulating hemocytes. No significant difference in transcript number was seen for the gills and heart of *Vibrio*-challenged animals, despite the downward trend within these tissues 4 h after injection. For these tissues in the *Vibrio*-treated animals, lysozyme transcript numbers began increasing after 4 h and had recovered to similar levels as the saline-injected animals by 12–24 h post-injection.

Lysozyme transcripts in the muscle at the site of injection displayed a very different pattern over time from the gills, heart, hemolymph and lymphoid organ. At 4 h after injection both saline and *Vibrio*-treated groups had higher lysozyme signals compared to early (0.25 h) transcript numbers. The number of lysozyme transcripts in muscle continued to increase to a maximum at 12 h in *Vibrio*-injected animals, but not in saline controls, such that at 12 h post-injection there were significantly ($p \leq 0.01$) higher numbers of transcripts in the muscle of animals injected with bacteria, compared to saline-injected animals. Significantly higher lysozyme transcript levels were measured in the muscle until the conclusion of the experiment at 48 h post-injection. Levels of lysozyme transcripts in hepatopancreas tissue were equivalent for all time-points between the 2 treatments.

When comparing the mean level of lysozyme expression by tissue across all of the tested time-points, the lymphoid organ contained a significantly higher number of lysozyme transcripts ng^{-1} RNA compared to the gills and the heart, and each of these tissues was significantly higher in expression than the hepatopancreas or muscle. In this experiment, circulating hemocytes were equivalent in lysozyme transcript concentration compared to those measured in the gills and heart. Significant differences between tissues were resolved using a 2-way ANOVA (treatment and tissue; $p \leq 0.05$) and multiple comparison using the Holm–Sidak multiple comparison test.

3.4. Artificial neural network analysis of lysozyme time-course data

Artificial neural networks (ANNs) are particularly useful for analyzing complex nonlinear biological data and identifying the relative contributions of each input variable to a measured output [34]. In the present study, significant differences were always identified between tissue types using a 3-way mixed model ANOVA when the complete, multi-variable real-time PCR data set was transformed in various ways, but treatment effects and especially, time-point-specific significant differences varied depending on how the lysozyme transcript data were transformed. We used ANN analysis to identify the relative weights that each variable contributed to the total observed variation in the lysozyme data to confirm that treatment and time-point after injection were important to the observed outcomes. The multi-layer feed-forward network devolved the 9 input variables of the input layer to 5 hidden nodes in the hidden layer. The correlation coefficients for the observed versus predicted data were calculated from each analysis. The mean correlation coefficient for the 10 ANNs was 0.9490 ± 0.0004 SD. Sensitivity analysis was also conducted for each ANN on each of the 9 input variables (time after injection, treatment, total hemocyte count, and each of the tested tissues). ANN analysis indicated that each of the input variables contributed to the overall variance observed (Fig. 4). The time post-injection ($20.652\% \pm 0.611\%$) and the effect of treatment (*Vibrio* injected or control saline injected; $16.367\% \pm 1.221\%$) contributed the largest percentage of variance. Each of the individual tissues contributed a lesser amount to the observed variance (6.355–9.796%).

4. Discussion

The present study provides a quantitative profile of the number and distribution of hemocyte lysozyme transcripts during the course of a successful immune response to a pathogenic bacterium. The rapid and sustained drop in total circulating hemocyte numbers accompanied by a significant and persistent increase in lysozyme transcripts in the muscle suggests that as bacteria disseminate via circulation, hemocytes traffic into tissues following a predictable pattern. Several other studies have shown that hemocytes rapidly traffic to the site of injection of bacteria where they become increasingly phagocytic [2], and lyse and/or degranulate to release immune effectors such as antimicrobial peptides [12,36], prophenoloxidase [37], transglutaminase activators [38], and lysozyme. Based on the results of the present study, we suggest that the decreased lysozyme signature seen in tissues (and circulating hemocytes) during the early (<12 h) phase of infection is due to massive granular hemocyte infiltration at the site of injection. As noted previously, the muscle at the site of *Vibrio* injection increased in lysozyme mRNA

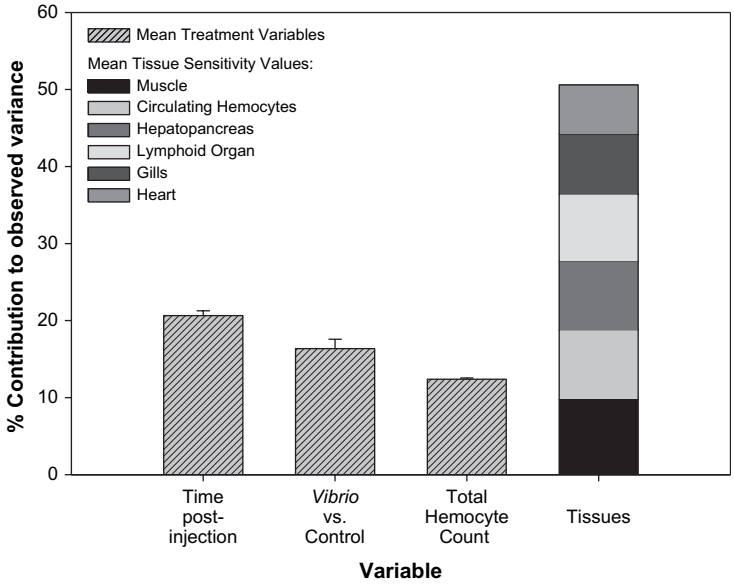

Fig. 4. Artificial neural networks. Artificial neural networks (ANN; $n = 10$) were used to estimate the relative contribution of each variable to the overall signal observed in lysozyme expression. Each input variable had an important effect on the outcome. Mean sensitivity values (±SE) for time after injection ($20.6 \pm 0.61\%$), *Vibrio* injection ($16.37 \pm 1.22\%$), and total hemocyte count ($12.38 \pm 0.17\%$) are shown separately. The contribution of each tissue is shown in the column labeled tissues and represented $50.6 \pm 2.39\%$ of the total variance in aggregate. The mean correlation coefficient for 10 ANNs was 0.949 ± 0.003.

concentration and peaked at ~20-fold higher levels 12 h post-injection. These results are consistent with the findings of Muñoz et al. [12], who examined penaeidin expression in *L. vannamei* injected with *Vibrio alginolyticus*. Using a non-quantitative approach, these authors detected a sharp initial decrease in penaeidin-expressing hemocytes (both in circulation and within tissues) during the first 12 h post-challenge. By 6–12 h after injection of *Vibrio* into the tail muscle of shrimp, large numbers of penaeidin-positive hemocytes were visualized at the site of injection, while control animal muscle and other spatially separate tail regions of *Vibrio*-injected shrimp contained very few penaeidin-expressing hemocytes. In the same study, THC declined within 12 h of injection and recovered to pre-injection levels by 48–72 h after injection. Interpreting the results of Muñoz et al. [12] and the present study in the context of bacterial clearance from circulation and accumulation within tissues, it seems clear that large numbers of hemocytes are recruited to the site of injection.

Supporting this assertion, Burgents et al. [6], using real-time PCR and selective plating, confirmed that greater than 50% of an injected dose of bacteria was still sequestered at the site of injection 4 h later, using the same species of shrimp and bacterium and the same injection dose and route of introduction as the present work. While penaeidin protein expression is confined to granular hemocytes [36], lysozyme transcripts are easily detected by in situ hybridization in both hyaline and granular hemocytes, although the latter subset is more intensely stained. The simultaneous decrease in THC and in lysozyme transcripts in the first 4 h post-injection supports the conclusion of Muñoz et al. [12] that granular hemocytes preferentially mobilize to the site of injection. Furthermore, high lysozyme transcript numbers persisted at the injection site, suggesting that granular hemocytes localized to the muscle remain intact for at least 48 h after mobilization, even during the period in which lysozyme transcripts in circulating hemocytes increase.

Measurement of lysozyme transcripts in tissues other than the muscle of *Vibrio*-injected shrimp illuminates hemocyte trafficking throughout the animal and suggests that, after 12 h, increases in lysozyme transcripts in the peripheral tissues are due to highly upregulated transcription for this gene in the remaining hemocytes or, potentially, new, actively transcribing hemocytes that are released from the hematopoietic tissue. THC did not indicate the release of large numbers of immature hemocytes, however, as circulating cells were significantly different at 48 h after injection of bacteria. Whereas saline-injected shrimp showed slight increases in lysozyme transcript numbers in various tissues, *Vibrio*-injected animals experienced a profound drop in measurable transcripts in the gill, heart and lymphoid organ

between 1 and 4 h. At 4 h after *Vibrio* injection, lysozyme transcript levels reached minimum values in the gill, heart, and lymphoid organ that were 4–8 times lower than those recorded for these tissues at 1 h post-injection. de Lorgeril et al. [26] reported very similar lysozyme expression from *L. stylirostris* infected with *Vibrio* and speculated that this response was due to granular hemocytes leaving the circulation and infiltrating tissues, or due to individual hemocyte regulation of lysozyme transcription.

A quantitative assessment of bacterial localization and bacteriostasis in *L. vannamei* [6] revealed that the lymphoid organ was distinct from the gills, hepatopancreas, heart, and hemolymph, in that it was the only tissue that preferentially accumulated (or produced) nonculturable bacteria. The authors interpreted that the transition from a culturable to a nonculturable state reflected bacteriostasis induced by the host within the lymphoid organ. They suggested that the lymphoid organ is specialized for the recognition and killing of infecting bacteria. The present study supports this assertion by demonstrating that among the tissues assayed for lysozyme transcripts, the lymphoid organ stood out from the other tissues in its overall higher level of lysozyme mRNA expression (see Fig. 3). Lysozyme protein antibacterial activity has been previously demonstrated from shrimp in a number of studies [23–25].

Examination of the lysozyme transcript data from the control animals, coupled with THC for the relevant timepoints, indicates that there is a possible ''wounding response'' that occurs after injection of saline. Notably, THC of control animals declined by approximately 37%, presumably as cells were recruited to the site of injection (wound). Concurrently, lysozyme transcripts increased in the muscle near the wound between 1 and 4 h by approximately 5-fold, and returned to pre-exposure levels by 12 h in animals receiving a sterile-saline injection. This transitory increase in lysozyme transcript levels demonstrates that hemocytes traffic to the site of injection in response to injury, and that this response is magnified by the presence of bacteria. It is likely that this response is part of a larger systemic mobilization of cellular and humoral immune components that in a normal, non-sterile wound would subsequently be used for bacterial detection and elimination.

In situ hybridization with *L. vannamei*-specific lysozyme antisense probes confirmed that mRNA expression for the gene was only present in cells that morphologically resembled circulating hemocytes. Highly granular hemocytes exhibited the strongest hybridization signals, and this may indicate that lysozyme transcripts were preferentially produced in these cells. Quantitative lysozyme transcriptional differences among hemocyte subsets may be useful for ultimately estimating subset abundance of hemocytes within tissues, and provide additional insights into subset trafficking and a finer dissection of the role that each cell type plays in the immune response. It was not possible in these experiments to strictly correlate hemocyte abundance (estimated from lysozyme signal) with THC because of the differences noted in subset lysozyme expression. Additionally, it is possible, albeit unlikely, that other tissues that were not sampled, such as the eyestalk or hematopoietic organ, could contain lysozyme transcripts not directly attributable to hemocytes. Low hemocyte numbers in the gills are likely an artifact of histological processing, as fresh gill preparations contain large numbers of hemocytes, and as a tissue, the gills have relatively high lysozyme expression, presumably due to their high concentrations of hemocytes. Likewise, fixed phagocytes derived from circulating hyaline hemocytes and phagocytic reserve cells of hematopoietic origin [11] cannot be differentiated from circulating hemocytes trapped within tissues by lysozyme real-time PCR.

In summary, we examined the gene expression of lysozyme within tissues of the penaeid shrimp, *L. vannamei*, and evaluated changes in transcription during the time-course of a successful immune response to injection of a pathogenic bacterium, *V. campbellii*. These results suggest that hemocyte migration toward the site of injection (wound) occurs rapidly after the body is compromised and that high concentrations of lysozyme-expressing hemocytes remained at that location for at least 48 h after challenge. Lysozyme expression data supported the findings of Burgents et al. [6] and van de Braak et al. [9] that the lymphoid organ of penaeid shrimp is an important location for bacteria–hemocyte interactions. Continued research in this area should focus on elucidating the factors that mediate hemocyte chemotaxis and the regulatory mechanisms governing tissue, hemocyte, and bacteria interactions.

Acknowledgments

This report is based upon research supported by the National Science Foundation under grants IBN-0212921 and DBI-0244007. We thank Dr. Craig Browdy, Sarah Prior, and the Waddell Mariculture Center, South Carolina Department of Natural Resources (SCDNR), for providing *L. vannamei* used in these experiments. The expertise of Dr. Margaret Ryan and Dr. Nora B. Terwilliger of the Oregon Institute of Marine Biology, and Yvonne Bobo of SCDNR was invaluable for the in situ hybridization portion of this work. We acknowledge Dr. Allan Strand for

expertise in statistical analyses and Dr. Robert Chapman for training in neural networks analysis. This is Contribution No. 292 of the Grice Marine Laboratory, College of Charleston.

References

[1] Vázquez L, Maldonado G, Agundis C, Pérez A, Cooper EL, Zenteno E. Participation of a sialic acid-specific lectin from freshwater prawn *Macrobrachium rosenbergii* hemocytes in the recognition of non-self cells. J Exp Zool 1997;279:265–72.
[2] Martin GG, Poole D, Poole C, Hose JE, Arias M, Reynolds L, et al. Clearance of bacteria injected into the hemolymph of the penaeid shrimp, *Sicyonia ingentis*. J Invertebr Pathol 1993;62:308–15.
[3] Muñoz M, Cedeño R, Rodríguez J, van der Knaap WPW, Mialhe E, Bachère E. Measurement of reactive oxygen intermediate production in haemocytes of the penaeid shrimp, *Penaeus vannamei*. Aquaculture 2000;191:89–107.
[4] Fontaine CT, Lightner DV. Observations on the process of wound repair in penaeid shrimp. J Invertebr Pathol 1973;22:23–33.
[5] Söderhäll K, Cerenius L. Crustacean immunity. Annu Rev Fish Dis 1992;2:3–23.
[6] Burgents JE, Burnett LE, Stabb EV, Burnett KG. Localization and bacteriostasis of *Vibrio* introduced into the Pacific white shrimp, *Litopenaeus vannamei*. Dev Comp Immunol 2005;29:681–91.
[7] Martin GG, Kay J, Poole D, Poole C. In vitro nodule formation in the ridgeback prawn, *Sicyonia ingentis*, and the American lobster, *Homarus americanus*. Invertebr Biol 1998;117:155–68.
[8] Martin GG, Quintero M, Quigley M, Khosrovian H. Elimination of sequestered material from the gills of decapod crustaceans. J Crust Biol 2000;20:209–17.
[9] van de Braak CB, Botterblom MH, Taverne N, van Muiswinkel WB, Rombout JH, van der Knaap WP. The roles of haemocytes and the lymphoid organ in the clearance of injected *Vibrio* bacteria in *Penaeus monodon* shrimp. Fish Shellfish Immunol 2002;13:293–309.
[10] Smith VJ, Söderhäll K. Induction of degranulation and lysis of haemocytes in the freshwater crayfish, *Astacus astacus* by components of the prophenoloxidase activating system in vitro. Cell Tissue Res 1983;233:295–303.
[11] Johnson PT. A review of fixed phagocytic and pinocytotic cells of decapod crustaceans, with remarks on hemocytes. Dev Comp Immunol 1987;11:679–704.
[12] Muñoz M, Vandenbulcke F, Saulnier D, Bachère E. Expression and distribution of penaeidin antimicrobial peptides are regulated by haemocyte reactions in microbial challenged shrimp. Eur J Biochem 2002;269:2678–89.
[13] Martin GG, Graves BL. Fine structure and classification of shrimp hemocytes. J Morphol 1985;185:339–48.
[14] Hose JE, Martin GG, Gerard AS. A decapod hemocyte classification scheme integrating morphology, cytochemistry, and function. Biol Bull 1990;178:33–45.
[15] Rodriguez J, Boulo V, Mialhe E, Bachère E. Characterisation of shrimp haemocytes and plasma components by monoclonal antibodies. J Cell Sci 1995;108:1043–50.
[16] Sung HH, Sun R. Use of monoclonal antibodies to classify hemocyte subpopulations of tiger shrimp (*Penaeus monodon*). J Crust Biol 2002;22:337–44.
[17] Winotaphan P, Sithigorngul P, Muenpol O, Longyant S, Rukpratanporn S, Chaivisuthangkura P, et al. Monoclonal antibodies specific to haemocytes of black tiger prawn *Penaeus monodon*. Fish Shellfish Immunol 2005;18:189–98.
[18] Zhang Z, Zhan W, Xue Y, Xing J. Antigenic cross-reactivity of crustacean haemocytes using monoclonal antibodies produced against haemocytes of shrimp (*Litopenaeus vannamei*). Fish Shellfish Immunol 2004;16:71–3.
[19] He N, Qin Q, Xu X. Differential profile of genes expressed in hemocytes of white spot syndrome virus-resistant shrimp (*Penaeus japonicus*) by combining suppression subtractive hybridization and differential hybridization. Antivir Res 2005;66:39–45.
[20] Söderhäll I, Bangyeekhun E, Mayo S, Söderhäll K. Hemocyte production and maturation in an invertebrate animal; proliferation and gene expression in hematopoietic stem cells of *Pacifastacus leniusculus*. Dev Comp Immunol 2003;27:661–72.
[21] Gross PS, Bartlett TC, Browdy CL, Chapman RW, Warr GW. Immune gene discovery by expressed sequence tag analysis of hemocytes and hepatopancreas in the Pacific White Shrimp, *Litopenaeus vannamei*, and the Atlantic White Shrimp, *L. setiferus*. Dev Comp Immunol 2001;25:565–77.
[22] Prager EM, Jollès P. Animal lysozymes *c* and *g*: an overview. In: Jollès P, editor. Lysozymes: model enzymes in biochemistry and biology. Basel, Switzerland: Birkhäuser Verlag; 1996. p. 9–31.
[23] de-la-Re-Vega E, García-Galaz A, Díaz-Cinco ME, Sotelo-Mundo RR. White shrimp (*Litopenaeus vannamei*) recombinant lysozyme has antibacterial activity against Gram negative bacteria: *Vibrio alginolyticus*, *Vibrio parahemolyticus* and *Vibrio cholerae*. Fish Shellfish Immunol 2006;20:405–8.
[24] Sotelo-Mundo RR, Islas-Osuna MA, de-la-Re-Vega E, Hernández-López J, Vargas-Albores F, Yepiz-Plascencia G. cDNA cloning of the lysozyme of the white shrimp *Penaeus vannamei*. Fish Shellfish Immunol 2003;15:325–31.
[25] Hikima S, Hikima J, Rojtinnakorn J, Hirono I, Aoki T. Characterization and function of kuruma shrimp lysozyme possessing lytic activity against *Vibrio* species. Gene 2003;316:187–95.
[26] de Lorgeril J, Saulnier D, Janech MG, Gueguen Y, Bachère E. Identification of genes that are differentially expressed in hemocytes of the Pacific blue shrimp (*Litopenaeus stylirostris*) surviving an infection with *Vibrio penaeicida*. Physiol Genomics 2005;21:174–83.
[27] Stabb EV, Ruby EG. RP4-based plasmids for conjugation between *Escherichia coli* and members of the *Vibrionaceae* Methods in enzymology: bacterial pathogenesis, Part C: identification, regulation and function of virulence factors. In: Clark VL, Bavoil PM, editors. Elsevier Science and Technology Books; 2002. p. 413–26.
[28] Mikulski CM, Burnett LE, Burnett KG. The effects of hypercapnic hypoxia on the survival of shrimp challenged with *Vibrio parahaemolyticus*. J Shellfish Res 2000;19:301–11.

[29] Gomez-Gil B, Soto-Rodríguez S, García-Gasca A, Roque A, Vazquez-Juarez R, Thompson FL, et al. Molecular identification of *Vibrio harveyi*-related isolates associated with diseased aquatic organisms. Microbiology 2004;150:1769–77.
[30] Vargas-Albores F, Guzmán MA, Ochoa JL. An anticoagulant solution for haemolymph collection and prophenoloxidase studies of penaeid shrimp (*Penaeus californiensis*). Comp Biochem Physiol A Physiol 1993;106:299–303.
[31] Bustin SA. Absolute quantification of mRNA using real-time reverse transcription polymerase chain reaction assays. J Mol Endocrinol 2000;25:169–93.
[32] Terwilliger NB, Ryan MC, Towle D. Evolution of novel functions: cryptocyanin helps build new exoskeleton in *Cancer magister*. J Exp Biol 2005;208:2467–74.
[33] Hasson KW, Hasson J, Aubert H, Redman RM, Lightner DV. A new RNA-friendly fixative for the preservation of penaeid shrimp samples for virological detection using cDNA genomic probes. J Virol Methods 1997;66:227–36.
[34] Almeida JS. Predictive non-linear modeling of complex data by artificial neural networks. Curr Opin Biotechnol 2002;13:72–6.
[35] R Development Core Team. R. A language and environment for statistical computing, http://www.R-project.org. v. 1.9.1.
[36] Destoumieux D, Muñoz M, Cosseau C, Rodriguez J, Bulet P, Comps M, et al. Penaeidins, antimicrobial peptides with chitin-binding activity, are produced and stored in shrimp granulocytes and released after microbial challenge. J Cell Sci 2000;113:461–9.
[37] Sritunyalucksana K, Söderhäll K. The proPO and clotting system in crustaceans. Aquaculture 2000;191:53–69.
[38] Omori SA, Martin GG, Hose JE. Morphology of hemocyte lysis and clotting in the ridgeback prawn, *Sicyonia ingentis*. Cell Tissue Res 1989;255:117–23.